

Functional renormalization group at finite density and Bose condensation

Eirik E. Svanes, Jens O. Andersen

Department of Physics, Norwegian University of Science and Technology, Høgskoleringen 5, N-7491 Trondheim, Norway

Abstract

We discuss the functional renormalization group and pion condensation in the presence of a finite isospin chemical potential μ_I . We calculate the phase diagram as function of temperature T and μ_I . While the exact effective average action is invariant under certain gauge transformations, the effective action in the local-potential approximation is not. As a consequence, the critical chemical potential μ_I^c for Bose-Einstein condensation at $T = 0$ is no longer equal to the mass of the condensing mode. We discuss possible solutions to this problem.

Keywords: Pion condensation, functional renormalization group, finite-temperature field theory

1. Introduction

One of the goals of heavy-ion collisions is to create energy densities and temperatures high enough to create a quark-gluon plasma and to study part of the phase diagram of quantum chromodynamics (QCD). The attempts to understand the phase structure of QCD, together with the sign problem at nonzero baryon chemical potential μ_B , have triggered interest in several QCD-like theories. These include QCD at nonzero isospin density [1], QCD with adjoint quarks, and two-color QCD [2]. A common feature of these theories is that they are free of the sign problem. On one hand this admits their straightforward simulation using lattice Monte-Carlo techniques and serves as a check of these methods against model-independent predictions of chiral perturbation theory. On the other hand, it allows a direct test of various model calculations at high temperature and/or density where chiral perturbation theory is not applicable. Hence the study of QCD-like theories contributes to our understanding of the physics of strongly-coupled gauge theories at nonzero temperature and density.

In the present paper, we consider the simpler problem of pion condensation in the presence of a finite chemical potential for isospin μ_I using the linear sigma model. Lattice simulations [3, 4, 5] suggest that there is a deconfinement transition of pions at high temperature and low density, and Bose-Einstein condensation of charged pions at high isospin density and low temperature. In fact, the deconfinement transition and the transition to a charged pion condensate seem to coincide. The deconfinement transition is found by measuring the Polyakov loop and the measurements show a sharp increase (indicating deconfinement) at approximately the same temperature as the

Email addresses: `svanes@stud.ntnu.no` (Eirik E. Svanes), `andersen@tf.phys.ntnu.no` (Jens O. Andersen)

onset of pion condensation. Pion condensation at finite μ_I has also been studied using chiral perturbation theory [1, 6, 7], ladder QCD [8], the chiral quark model [9, 10], the linear sigma model [11, 12, 13, 15, 16, 17], the NJL model [14, 18, 19, 20, 21, 22, 23, 24], and Polyakov-loop NJL (PNJL) models [25, 26]. The PNJL model suggests that deconfinement and the onset of Bose-Einstein condensation are two different transitions. Finally, the possibility of a BEC-BCS crossover from a Bose condensate to superconducting state has been investigated [27]. Note that this is not a phase transition since there is no global order parameter that distinguishes the crossover. Rather, it is a qualitative change from a pion condensate of tightly bound quarks to weakly bound Cooper pairs as the isospin density increases.

The model calculations are typically of mean-field type and going beyond mean field is the next step in the study of these models. In order to do so we apply the functional renormalization group (FRG) [28, 29, 30, 31, 32, 33, 34, 35, 36]. The paper is based on Ref. [37]. The functional renormalization group is a nonperturbative method, with a wide range of applicability. It is an alternative, but equivalent formulations to Wilson's ideas from the 1970s. It has been used successfully to calculate critical exponents for phase transitions [38] and to map out the phase diagram as function of temperature and baryon chemical potential [39, 40, 41, 42] as well as the calculations of thermodynamic functions [43] and momentum-dependent correlation functions at high temperature [44, 45].

2. Flow equation and derivative expansion

One implementation of the renormalization group ideas is based on the effective average action $\Gamma_k[\phi]$ as proposed by Wetterich [28]. The effective average action is a functional of a set of fields denoted by ϕ and satisfies a flow equation which is an integro-differential equation. The subscript k indicates that all momentum modes q between the UV cutoff of the theory, Λ , and k have been integrated out. When $k = \Lambda$, no momentum modes have been integrated out and the effective action is equal to the classical action of the theory, i.e. $\Gamma_\Lambda[\phi] = S[\phi]$. When $k = 0$, all modes have been integrated out and $\Gamma_0[\phi]$ is equal to the full quantum effective action. All quantum and thermal fluctuations from $k = 0$ up to $k = \Lambda$ have then been included. The exact flow equation for $\Gamma_k[\phi]$ is

$$\partial_k \Gamma_k[\phi] = \frac{1}{2} \text{Tr} \left[\partial_k R_k(q) (\Gamma_k^{(2)} + R_k(q))_{q,-q}^{-1} \right], \quad (1)$$

where the superscript n on $\Gamma_k[\phi]$ means the n 'th functional derivative and the trace is over the spacetime momenta q , and indices of the inverse propagator matrix. The function $R_k(q)$ is a regulator and is introduced in order to implement the renormalization group ideas: $R_k(q)$ is large for $q < k$ and small for $q > k$ whenever $0 < k < \Lambda$, and $R_\Lambda(q) = \infty$. These properties ensure that the modes below k are heavy and decouple, and only the modes between k and the UV cutoff Λ are light and integrated out. The diagrammatic representation of the flow equation is shown in Fig. 1.

The choice of regulator has been discussed extensively in the literature [46, 47, 48]. We employ the regulator which is given by

$$R_k(q) = (k^2 - \mathbf{q}^2) \Theta(k^2 - \mathbf{q}^2). \quad (2)$$

Note that this is not the precise regulator described in [47] as it only involves the three-momentum \mathbf{q} and is rotationally invariant, i.e. we have omitted the zeroth component of the four-vector q . This regulator is particularly convenient in practical calculations since one can carry out the integral over three-momenta exactly and this turns the flow equation into a partial differential equation.

$$\partial_k \Gamma_k = \frac{1}{2} \text{ (circle with a dot) }$$

Figure 1: Diagrammatic representation of the exact flow equation for the effective action $\Gamma_k[\phi]$. The line denotes the exact field-dependent propagator and the circle denotes an insertion of the regulator $R_k(q)$.

The starting point of our discussion is the classical action $S[\phi]$. In the present case we consider N complex scalar fields with a quartic self-interaction and $S[\phi]$ reads

$$S[\phi] = \int_0^\beta d\tau \int_{\mathbf{q}} \left\{ (\partial_\mu \Phi_i^\dagger)(\partial_\mu \Phi_i) + m^2 \Phi_i^\dagger \Phi_i - \frac{H}{\sqrt{2}} [\Phi_1^\dagger + \Phi_1] + V(\phi) \right\}, \quad (3)$$

where the classical potential is

$$V(\phi) = \frac{g^2}{2N} (\Phi_i^\dagger \Phi_i)^2, \quad (4)$$

and where $i = 1, 2, 3 \dots N$. The complex fields Φ_i are written in terms of real fields, $\Phi_i = (\phi_{2i-1} + i\phi_{2i})/\sqrt{2}$. We identify ϕ_1 with σ , π^\pm with $(\phi_2 \pm i\phi_3)/\sqrt{2}$, and $\phi_4, \phi_5, \dots, \phi_{2N}$ with $2N-3$ neutral π^0 . The parameter H breaks the $O(2N)$ symmetry explicitly to $O(2N-1)$ and gives rise to nonzero pion masses. The parameter m^2 is negative in the remainder to ensure spontaneous symmetry breaking in the vacuum for $H = 0$.

A chemical potential μ_i that corresponds to the conserved charge of the $U(1)$ -symmetry $\Phi_i \rightarrow e^{i\alpha} \Phi_i$ is introduced by the replacement $\partial_0 \Phi_i \rightarrow (\partial_0 - \mu_i) \Phi_i$. The chemical potential acts as the zeroth component of an Abelian gauge field. The classical action is therefore invariant under the gauge transformation

$$\Phi_i \rightarrow e^{i\alpha} \Phi_i, \quad (5)$$

$$\mu_i \rightarrow \mu_i + \partial_0 \alpha. \quad (6)$$

The introduction of the isospin chemical potential μ_I reduces the symmetry to $O(2) \times O(2N-2)$ if $H = 0$, otherwise to $O(2) \times O(2N-3)$. Chiral symmetry is broken in the vacuum, either spontaneously or explicitly by a vacuum expectation value ϕ_0 for ϕ_1 . We also allow for a pion condensate by a nonzero value ρ_0 of ϕ_2 . A pion condensate breaks the $O(2)$ -symmetry.

After having introduced the isospin chemical potential μ_I , the classical potential is ¹

$$U_\Lambda(\phi) = \frac{1}{2} m_\Lambda^2 (\phi_0^2 + \rho_0^2) - \frac{1}{2} \mu_I^2 \rho_0^2 + \frac{g_\Lambda^2}{8N} (\phi_0^2 + \rho_0^2)^2 - H \phi_0, \quad (7)$$

where the subscript Λ is a reminder that the classical potential equals the boundary condition for the effective potential $U_k(\phi)$ (see below).

¹Note that in the vacuum and for $H = 0$, the potential depends only on combination $\phi_0^2 + \rho_0^2$. One can therefore use the symmetry to rotate away ρ_0 . This is in accord with the Vafa-Witten theorem [49] that states that parity cannot be spontaneously broken in the vacuum.

The exact flow equation (1) cannot not be solved so one must resort to approximations. The derivative expansion is a commonly used approximation and reads

$$\Gamma_k[\phi] = \int \left[Z_k^{\Phi_1} \left(\nabla \Phi_1^\dagger \right) \left(\nabla \Phi_1 \right) + Z_k^{\Phi_2} \left(\partial_0 - \mu_I \Phi_1^\dagger \right) \left(\partial_0 - \mu_I \Phi_1 \right) + Z_k^{\Phi_3} \left(\nabla \Phi_3^\dagger \right) \left(\nabla \Phi_3 \right) + \dots + U_k(\phi) + \dots \right], \quad (8)$$

where $Z_k^{\Phi_i}$ are wavefunction renormalization constants and $U_k(\phi)$ is the scale-dependent effective potential that depends on the classical fields collectively denoted by ϕ . Note that the $Z_k^{\Phi_i}$'s are in principle different since Lorentz invariance is broken due to both finite temperature and finite density. The ellipsis indicate higher-order operators including derivatives such as $\Phi^\dagger \Phi (\nabla \Phi^\dagger \nabla \Phi)$. In the local-potential approximation, we set $Z_k^{\Phi_i} = 1$ and omit such higher-order operators. In this approximation, the flow equation is an integro-differential equation for $U_k(\phi)$ ².

The flow equation for the effective potential $U_k(\phi)$ is derived in the Appendix and reads

$$\partial_k U_k(\phi) = \frac{4k^d v_{d-1}}{(d-1)} \left\{ \left[\sum_{i=1}^3 \frac{(1 + 2n(\sqrt{P_i})) R_i}{2\sqrt{P_i}} \right] + (2N-3) \frac{1 + 2n(\omega_3)}{2\omega_3} \right\}, \quad (9)$$

where $d-1$ is the dimension of space, $v_d = [2^{d+1} \pi^{d/2} \Gamma(\frac{1}{2})]^{-1}$, $n(x) = 1/(e^{\beta x} - 1)$ is the Bose-Einstein distribution function, P_i and R_i are poles and residues defined in the Appendix. Moreover, $U_k(\phi)$ is a function of $\rho_1 = \frac{1}{2}\phi_0^2$ and $\rho_2 = \frac{1}{2}\rho_0^2$. We then introduce the shorthand notation $\partial_1 U_k(\phi) \equiv \partial U_k(\phi)/\partial \rho_1$, $\partial_2 U_k(\phi) \equiv \partial U_k(\phi)/\partial \rho_2$, and $\omega_3 = \sqrt{k^2 + \partial_1 U_k}$.

3. Numerical results and discussion

In this section, we solve the flow equation (9) numerically using a third-order Runge-Kutta method and discuss the resulting phase diagram. The boundary potential is given by Eq. (7), where we in remainder of this section set $N = 2$. and the parameters m_Λ^2 and g_Λ^2 are determined so that we reproduce the pion mass m_π , the sigma mass m_σ , and the pion decay constant f_π in the vacuum, i.e. for $T = \mu_I = 0$. In the vacuum we have $\phi_0 = f_\pi$ and $\rho_0 \equiv 0$. The k -dependent masses $m_{\pi,k}$ and $m_{\sigma,k}$ can be related to the effective potential at the k -dependent minimum $f_{\pi,k}$ as follows

$$m_{\pi,k}^2 = \left. \partial_1 \tilde{U}_k(\phi) \right|_{\phi_0=f_{\pi,k}, \rho_0=0} \quad (10)$$

$$\begin{aligned} m_{\sigma,k}^2 &= \left. \partial_1 \tilde{U}_k(\phi) \right|_{\phi_0=f_{\pi,k}, \rho_0=0} + \phi_0^2 \partial_1^2 \tilde{U}_k(\phi) \Big|_{\phi_0=f_{\pi,k}, \rho_0=0} \\ &= m_{\pi,k}^2 + \phi_0^2 \partial_1^2 \tilde{U}_k(\phi) \Big|_{\phi_0=f_{\pi,k}, \rho_0=0}, \end{aligned} \quad (11)$$

²Sometimes one further assumes that $U_k(\phi)$ takes a polynomial form and the partial differential equation (9) is turned into a set of coupled differential equations for the couplings.

where $\tilde{U}_k(\phi) = U_k(\phi) + H\phi_0$, i.e. the potential without the explicit symmetry breaking term. In particular, the physical pion and sigma masses, i.e. the masses for $k = 0$ are given by

$$m_\pi^2 = \left. \partial_1 \tilde{U}_0(\phi) \right|_{\phi_0=f_\pi, \rho_0=0} \quad (12)$$

$$m_\sigma^2 = \left. m_\pi^2 + \phi_0^2 \partial_1^2 \tilde{U}_0(\phi) \right|_{\phi_0=f_\pi, \rho_0=0}. \quad (13)$$

In Fig. 2 we show the real part of the scaled effective potential as function of $\phi_0^2/2\Lambda^2$ in the chiral

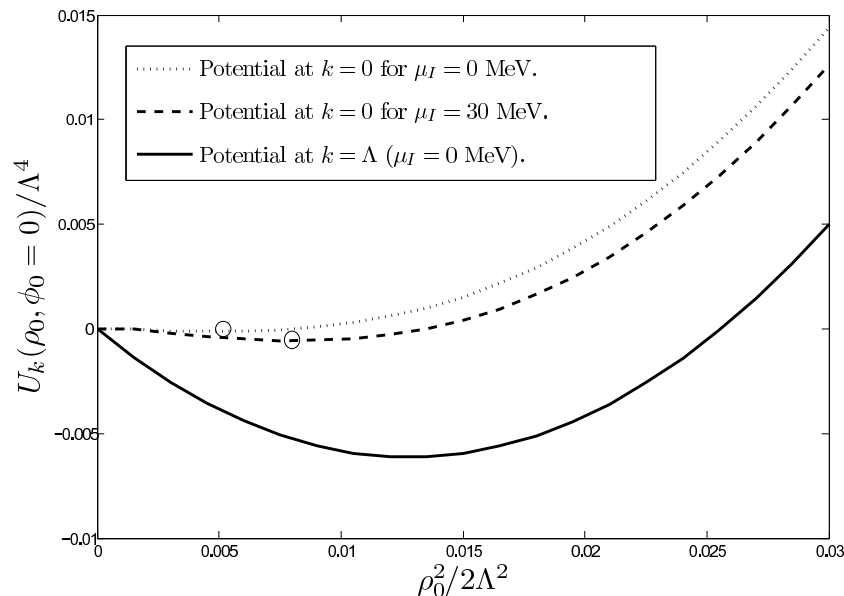


Figure 2: The real part of $U_k(\phi_0, \rho_0 = 0)/\Lambda^4$ as a function of $\phi_0^2/2\Lambda^2$ at $T = 0$ in the chiral limit. The potential is plotted for $k = \Lambda$, and for $k = 0$ in the case of $\mu_I = 0$ MeV and $\mu_I = 30$ MeV, where we have neglected the constant added to the potential by renormalization. We have used $m_\sigma = 400$ MeV and $f_\pi = 93$ MeV in order to tune the bare parameters of the potential at the cutoff $\Lambda = \sqrt{5}m_\sigma$. The minima of the renormalized potentials have been marked with transparent circles making them easier to see.

limit and for $T = 0$ at $\mu_I = 0$ and $\mu_I = 30$ MeV³.

We use the experimental value $f_\pi = 93$ MeV and $m_\sigma = 400$ MeV to tune the bare parameters in this case. We chose the cutoff $\Lambda^2 = 5m_\sigma^2$. This gives the values $m_\Lambda^2 = -0.96\Lambda^2$ and $g_\Lambda^2 = 37.56$. We find that the inclusion of a finite chemical potential has the effect of increasing the ρ_0 value for which $U_k(\phi)$ takes its minimum. We also see from the Fig. that the renormalization of $U_k(\phi)$ is large when integrating from $k = \Lambda$ down to $k = 0$.

In Fig. 3, we show the chiral condensate (dashed line) and pion condensate (solid line) as function of μ_I at zero temperature. In the chiral limit the charged pion condensate is the only condensate present at nonzero chemical potential when $T = 0$. We have used the parameters $f_\pi = 93$ MeV,

³Note that the effective potential in the broken phase has an imaginary part to the left of the minimum.

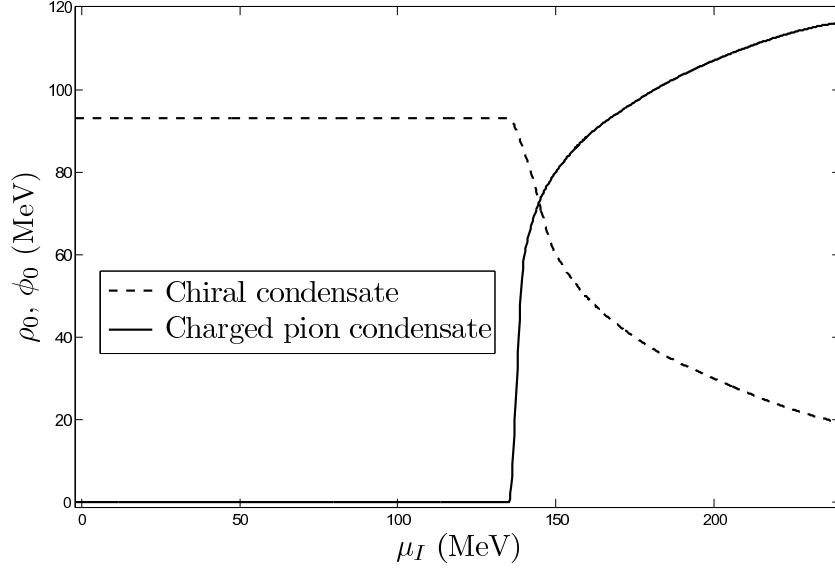


Figure 3: The chiral condensate and the charged pion condensate as a function of isospin chemical potential at the physical point at $T = 0$. We have used physical parameters $m_\sigma = 600$ MeV, $m_\pi = 140$ MeV, and $f_\pi = 93$ MeV, and set $\Lambda = 600$ MeV to tune the bare parameters.

$m_\sigma = 600$ MeV, $m_\pi = 140$ MeV, and $\Lambda = 600$ MeV. If we go to the physical point however, we see that a chiral condensate appears in the direction of ϕ_0 . For small chemical potentials, we find that the chiral condensate is the only existing condensate, that is, the minimum of $U_k(\phi)$ lies on the ϕ_0 -axis and no charged pion condensation takes place. As we increase the chemical potential however, the minimum eventually moves away from the ϕ_0 -axis and a charged pion condensate is formed, i.e. the chiral condensate is rotated into a condensate of π^+ and π^- . At $T = 0$ we find that this happens when the chemical potential is about the vacuum pion mass. This is in agreement with the results of e.g. [8, 10, 14, 15, 23] (but see the discussion below).

In Fig. 4, we plot the phase diagram as function of temperature and isospin chemical potential in the chiral limit (dashed line) and at the physical point (solid line). We use the same parameters as before. The phase diagram is in qualitative agreement with previous results [10, 14, 15, 23]. In particular, the phase transition to a condensate of pions is of second order and this is in accord with universality-class arguments. Note, however, that the critical chemical potential for $T = 0$ and at the physical point is different from the pion mass m_π and this is in disagreement with exact results. In fact, it can be shown that the critical chemical potential for Bose condensation at $T = 0$ is equal to the mass of the condensing mode. Using the bare parameters we found at $T = \mu_I = 0$, we see from Fig. 4 that we obtain a slightly different value for the critical chemical potential, namely $\mu_{I,c} = 135$ MeV. The reason we do not get the pion mass is that we are working in the local-potential approximation, where wave-function renormalization is neglected. Recall that to include an isospin chemical potential we should let $\partial_0 \Phi \rightarrow (\partial_0 - \mu_I) \Phi$, where we view the Lagrangian as a function of complex field variables. This term remains unrenormalized in the local-potential approximation and so the effective action is not gauge invariant under the transformations (5) - (6). This is in contrast to the full quantum effective action at $T = 0$ [50].

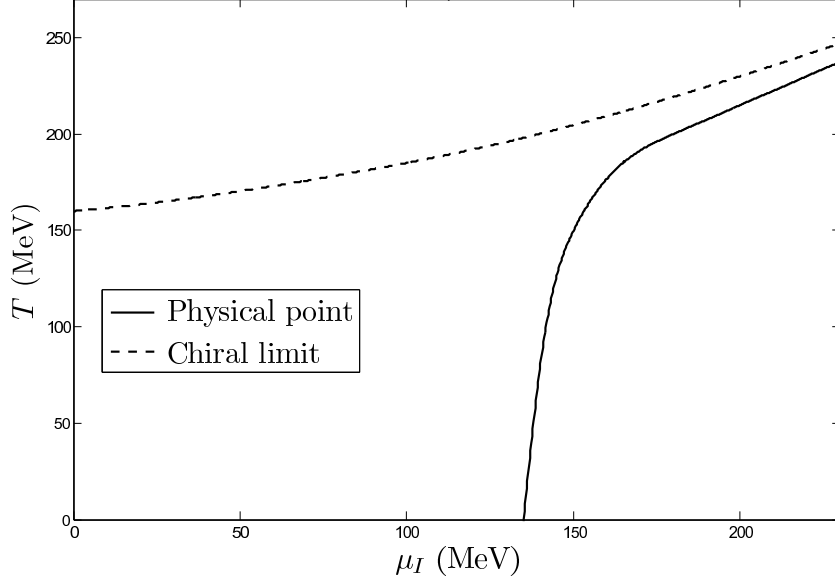


Figure 4: A plot showing the phase diagram for the charged pion condensate in the chiral limit and for the physical point. We have chosen physical values $f_\pi = 93$ MeV, $m_\sigma = 600$ MeV and $m_\pi = 140$ MeV ($m_\pi = 0$ in the chiral limit) in order to tune the bare parameters at $T = 0$. We have also set $\Lambda = 600$ MeV. The symmetric phase is above the lines, while the broken phase is below the lines.

A simple solution to this problem is to first solve the flow equation for the effective potential $U_k(\phi)$ in the absence of the isospin chemical potential and then gauge the effective action in the local-potential approximation by the substitution $\partial_0\Phi \rightarrow (\partial_0 - \mu_I)\Phi$. The effective potential at scale k may then be written as

$$U_k(\phi) = \tilde{U}_k(\phi) - \frac{1}{2}\mu_I^2\rho_0^2 - H\phi_0, \quad (14)$$

where $\tilde{U}_k(\phi)$ denotes the $O(4)$ -symmetric potential, i.e. the potential satisfying Eq. (9) with $\mu_I = 0$, that is Eq. (34) in the Appendix. We call this the $O(4)$ -approximation. In order to get a charged pion condensate at $k = 0$, one needs a negative partial derivative in the ρ_0 direction at the minimum of $U_k(\phi)$. When μ_I is just large enough for this to happen, we obtain

$$\begin{aligned} 0 &= \partial_2 U_{k=0}(\phi) \\ &= \partial_2 \tilde{U}_k(\phi) - \mu_I^2. \end{aligned} \quad (15)$$

Using the $O(4)$ -invariance of $\tilde{U}_k(\phi)$ and combining Eq. (15) with Eq. (12), this yields a critical chemical potential

$$\mu_I^c = m_\pi. \quad (16)$$

While the effective potential defined by Eq. (14) is in agreement with exact results, its dependence on the isospin chemical potential is of course trivial.

The large- N limit provides us with another flow equation for $U_k(\phi)$ which is independent of the chemical potential. It is given by Eq. (35) in the Appendix:

$$\partial_k U_k = \frac{8k^d v_{d-1}}{(d-1)} \frac{1 + 2n(\omega_3)}{2\omega_3}. \quad (17)$$

Thus using the same arguments as above, we obtain the critical chemical potential for pion condensation which is equal to the pion mass.

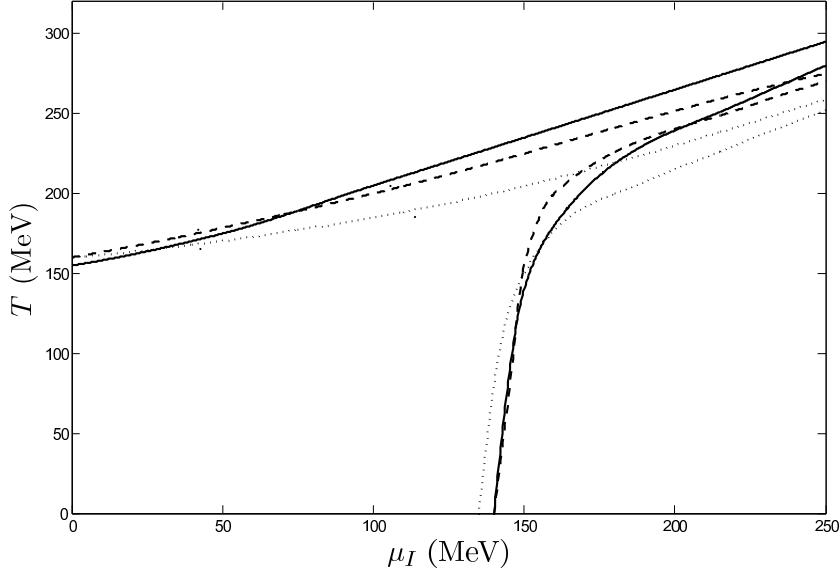


Figure 5: The phase diagram for the $O(4)$ -approximation (solid line) and the large- N limit (dashed line), where we have set $m_\pi = 140$ MeV, $f_\pi = 93$ MeV and $m_\sigma = 600$ MeV to determine the parameters at the cutoff $\Lambda = 1500$ MeV in the vacuum. We have also plotted the previous obtained phase diagram for comparison (dotted line).

In Fig. 5, we show the phase diagram obtained by solving the flow equation for $U_k(\phi)$ in the $O(4)$ -approximation and in the large- N limit. For comparison, we also show the phase diagram obtained by solving Eq. (9) and was shown in Fig. 4 for a different cutoff. In this plot, we used $\Lambda = 1500$ MeV. We would like to point out that both the $O(4)$ approximation and the large- N approximation yield a second-order transition.

In closing, we remark that it would be interesting to include the effects of wavefunction renormalization. This would lead to a set of coupled equations for $Z_k^{\Phi_i}$ and $U_k(\phi)$. Hopefully it would close the gap between the value $\mu_c = 135$ MeV obtained in this work and the exact result $\mu_c = m_\pi = 140$ MeV and so perhaps provide a practical solution to the problems of the local-potential approximation. Similarly, it would be interesting to apply the method to the chiral quark model. Since this model has quark degrees of freedom, one can simultaneously study the effects of a baryon and an isospin chemical potential. In particular, one can investigate the BEC-BCS transition as one increases μ_I .

Acknowledgments

The authors would like to thank Tomas Brauner and Holger Gies for useful discussions.

4. Appendix

In this Appendix, we derive the flow equation (9). The starting point is the exact flow equation (1) [28]

$$\partial_k \Gamma_k[\phi] = \frac{1}{2} \text{Tr} \left[\partial_k R_{k,q} (\Gamma_k^{(2)} + R_k)_{q,-q}^{-1} \right]. \quad (18)$$

The effective potential $U_k(\phi)$ is defined by evaluating the effective action $\Gamma_k[\phi]$ for space-time independent values of the fields, i. e.

$$U_k(\phi_{\text{uni}}) = \frac{1}{VT} \Gamma_k[\phi_{\text{uni}}], \quad (19)$$

where VT is the spacetime volume of the system and ϕ_{uni} is constant. Taking the derivative of Eq. (19) with respect to k , we obtain the RG-equation for the effective potential

$$\partial_k U_k(\phi_{\text{uni}}) = \frac{1}{2VT} \text{Tr} \left[\partial_k R_{k,q} (\Gamma_k^{(2)}[\phi_{\text{uni}}] + R_k)_{q,-q}^{-1} \right]. \quad (20)$$

In the remainder we drop the subscript uni. With $\Gamma_k[\phi]$ given as in Eq. (18), we find the Fourier transform of $\Gamma_k^{(2)}[\phi]$ to be

$$\Gamma_{k,i,j,q,q'}^{(2)} = (2\pi)^d \delta(q+q') \left[\frac{\partial^2 U_k}{\partial \phi_i \partial \phi_j} + \delta_{ij} q^2 - 2\mu_I q_0 (\delta_{j2} \delta_{i3} - \delta_{i2} \delta_{j3}) \right], \quad (21)$$

where d denotes the spacetime dimension and i, j are the indices of the propagator. Note that by the presence of the chemical potential, $\Gamma_{k,i,j,q,q'}^{(2)}$ is not a diagonal matrix. Also note that we cannot rotate the field vector $\phi = (\phi_1, \dots, \phi_{2N})$ to point in one specific direction as we do not have $O(2N)$ symmetry. This has been explicitly broken to a $O(2) \times O(2N-2)$ by the isospin chemical potential μ_I . The best we can do is to write $\phi = (\phi_0, 0, \rho_0, 0, \dots, 0)$ to incorporate both a chiral condensate and a charged pion condensate. This will also give rise to off-diagonal entries in the matrix. We now set $N = 2$ in order to simplify the derivation. Returning to a general N is straightforward.

We may assume, because of the $O(2) \times O(2)$ symmetry, that $U_k(\phi) = U_k(\rho_1, \rho_2)$ where

$$\begin{aligned} \rho_1 &= \frac{1}{2} \langle \phi_1^2 + \phi_4^2 \rangle \\ &= \frac{1}{2} \phi_0^2, \end{aligned} \quad (22)$$

$$\begin{aligned} \rho_2 &= \frac{1}{2} \langle \phi_2^2 + \phi_3^2 \rangle \\ &= \frac{1}{2} \rho_0^2. \end{aligned} \quad (23)$$

If we denote the fields by double indices $\phi = (\phi_{11}, \phi_{12}, \phi_{21}, \phi_{22})$, we can derive the identity

$$\frac{\partial^2 U_k}{\partial \phi_{ai} \partial \phi_{bj}} = \frac{\partial U_k}{\partial \rho_b} \delta_{ab} \delta_{ij} + \phi_{ai} \phi_{bj} \frac{\partial^2 U_k}{\partial \rho_a \partial \rho_b}. \quad (24)$$

The Fourier transform of $R_k(x-y)$ is $(2\pi)^d \delta(q+q') R_k(q) = R_{k,q,q'}$. If we add $\delta_{ij} R_{k,q,q'}$ to $\Gamma_{k,i,j,q,q'}^{(2)}$, we obtain the matrix

$$[\Gamma_k^{(2)} + R_k]_{q,q'} = (2\pi)^d \delta(q+q') \times \begin{pmatrix} \partial_1 U_k + 2\rho_1 \partial_1^2 U_k + F_k(q) & 0 & 2\sqrt{\rho_1 \rho_2} \partial_1 \partial_2 U_k & 0 \\ 0 & \partial_2 U_k + F_k(q) & -2\mu_I q_0 & 0 \\ 2\sqrt{\rho_1 \rho_2} \partial_1 \partial_2 U_k & 2\mu_I q_0 & \partial_2 U_k + 2\rho_2 \partial_2^2 U_k + F_k(q) & 0 \\ 0 & 0 & 0 & \partial_1 U_k + F_k(q) \end{pmatrix}, \quad (25)$$

where $F_k(q) = q^2 + R_k(q)$. Using the fact that the inverse in Fourier space satisfies

$$\int_{q'} F(q_1, q')_{ik} F^{-1}(q_2, q')_{kj} = (2\pi)^d \delta(q_1 - q_2) \delta_{ij}, \quad (26)$$

we may invert $[\Gamma_k^{(2)} + R_k]_{q,q'}$ to obtain the full k -dependent propagator. This may then be inserted into Eq. (20) in order to obtain the RG equation for the effective potential. Going to imaginary time we replace the integral over q_0 by a Matsubara sum $T \sum_n$. This yields

$$\begin{aligned} \partial_k U_k &= \frac{T}{2} \sum_n \int_{\mathbf{q}} \partial_k R_k \left[\left(2(q^2 + R_k + \partial_1 U_k + 2\rho_1 \partial_1^2 U_k)(q^2 + R_k + \partial_2 U_k + \rho_2 \partial_2^2 U_k) \right. \right. \\ &\quad \left. \left. - 4\rho_1 \rho_2 (\partial_1 \partial_2 U_k)^2 + (q^2 + R_k + \partial_2 U_k)(q^2 + R_k + 2\rho_2 \partial_2^2 U_k) + 4\mu_I^2 \omega_n^2 \right) \right] / \\ &\quad \left((q^2 + R_k + \partial_1 U_k + 2\rho_1 \partial_1^2 U_k) \left[(q^2 + R_k + \partial_2 U_k + 2\rho_2 \partial_2^2 U_k)(q^2 + R_k + \partial_2 U_k) + 4\mu_I^2 \omega_n^2 \right] \right. \\ &\quad \left. \left. - 4\rho_1 \rho_2 (\partial_1 \partial_2 U_k)^2 (q^2 + R_k + \partial_2 U_k) \right) + \frac{1}{q^2 + R_k + \partial_1 U_k} \right], \end{aligned} \quad (27)$$

where now $q^2 = \omega_n^2 + \mathbf{q}^2$ and $\omega_n = 2\pi nT$ denotes the Matsubara frequencies. The difference between this and arbitrary N is that there would be $2N - 3$ propagators of the form of the last term in the above expression.

Performing the integral over \mathbf{q} and returning to arbitrary N , we may simplify this by writing

$$\partial_k U_k = \frac{4Tk^d v_{d-1}}{(d-1)} \sum_n \left[\frac{N(\omega_n^2)}{D(\omega_n^2)} + \frac{2N-3}{\omega_n^2 + k^2 + \partial_1 U_k} \right], \quad (28)$$

where we have defined

$$\begin{aligned} N(\omega_n^2) &= 2(k^2 + \omega_n^2 + \partial_1 U_k + 2\rho_1 \partial_1^2 U_k)(k^2 + \omega_n^2 + \partial_2 U_k + \rho_2 \partial_2^2 U_k) - 4\rho_1 \rho_2 (\partial_1 \partial_2 U_k)^2 \\ &\quad + (k^2 + \omega_n^2 + \partial_2 U_k)(k^2 + \omega_n^2 + \partial_2 U_k + 2\rho_2 \partial_2^2 U_k) + 4\mu_I^2 \omega_n^2, \end{aligned} \quad (29)$$

$$\begin{aligned} D(\omega_n^2) &= (\omega_n^2 + k^2 + \partial_1 U_k + 2\rho_1 \partial_1^2 U_k) \left[(k^2 + \omega_n^2 + \partial_2 U_k + 2\rho_2 \partial_2^2 U_k)(k^2 + \omega_n^2 + \partial_2 U_k) \right. \\ &\quad \left. + 4\mu_I^2 \omega_n^2 \right] + 4\rho_1 \rho_2 (\partial_1 \partial_2 U_k)^2 (k^2 + \omega_n^2 + \partial_2 U_k). \end{aligned} \quad (30)$$

The denominator $D(\omega_n^2)$ is a third-degree polynomial in ω_n^2 . Writing out its roots P_i would take several pages. However, they can in principle be found, so we may for the sake of argument assume

that we have found them. If we denote by R_i the residue of the three poles P_i of $1/D(\omega_n^2)$, we may write

$$\frac{N(\omega_n^2)}{D(\omega_n^2)} = \sum_{i=1}^3 \frac{R_i}{\omega_n^2 + P_i}. \quad (31)$$

Summing over the Matsubara frequencies yields

$$\partial_k U_k = \frac{4k^d v_{d-1}}{(d-1)} \left\{ \sum_{i=1}^3 \left[\frac{(1 + 2n(\sqrt{P_i}))R_i}{2\sqrt{P_i}} \right] + (2N-3) \frac{1 + 2n(\omega_3)}{2\omega_3} \right\}. \quad (32)$$

Finding the poles P_i and the residues R_i is done numerically, by use of the residue function in Matlab.

In the case of zero chemical potential there is only the possibility of a chiral condensate. The situation is again $O(2N)$ symmetric. Eq. (31) then reduces to

$$\frac{N(\omega_n^2)}{D(\omega_n^2)} = \frac{1}{\omega_n^2 + k^2 + \partial_1 U_k(\rho_1) + 2\rho_1 \partial_1^2 U_k(\rho_1)} + \frac{1}{\omega_n^2 + k^2 + \partial_1 U_k(\rho_1)}, \quad (33)$$

The equation thus obtained is

$$\partial_k U_k = \frac{4k^d v_{d-1}}{(d-1)} \left\{ \frac{1 + 2n(\omega_1)}{2\omega_1} + (2N-1) \frac{1 + 2n(\omega_2)}{2\omega_2} \right\}, \quad (34)$$

where $\omega_1 = \sqrt{k^2 + \partial_1 U_k(\rho_1) + 2\rho_1 \partial_1^2 U_k(\rho_1)}$ and $\omega_2 = \sqrt{k^2 + \partial_1 U_k(\rho_1)}$.

The large- N limit of Eq. (32) is simple and reads

$$\partial_k U_k = \frac{8k^d v_{d-1}}{(d-1)} \frac{1 + 2n(\omega_3)}{2\omega_3}. \quad (35)$$

Note that the flow equation (35) is independent of the isospin chemical potential.

References

- [1] D. T. Son and M. A. Stephanov, Phys. Rev. Lett. **86** (2001) 592, e-Print: arXiv:hep-ph/0005225.
- [2] J. B. Kogut, M. A. Stephanov, and D. Toublan, Phys. Lett. B **464** (1999) 183, e-Print: arXiv:hep-ph/9906346; J. B. Kogut, M. A. Stephanov, D. Toublan, J. J. M. Verbaarschot, and A. Zhitnitsky, Nucl. Phys. B **582** (2000) 477, e-Print: arXiv:hep-ph/0001171.
- [3] J. B. Kogut and D. K. Sinclair, Phys. Rev. D **64** (2001) 034508; *ibid* D **66** 34505 (2002); *ibid* D **70** (2004) 094501.
- [4] S. Gupta, e-Print: arXiv:hep-lat/0202005.
- [5] P. de Forcrand, M. A. Stephanov, U. Wenger, PoS LAT2007 (2007) 237.
- [6] K. Splittorff, D. T. Son and M. Stephanov, Phys. Rev. D **64** (2001) 016003.

- [7] M. Loewe and C. Villavicencio, Phys. Rev. D **67** (2003) 074034; *ibid* D **70** (2004) 074005; *ibid* D **71** (2005) 094001.
- [8] A. Barducci, R. Casalbuoni, G. Pettini, and L. Ravagli, Phys. Lett. B **564** (2003) 217.
- [9] A. Jakovac, A. Patkos, Z. Szep, and P. Szepefalusy, Phys. Lett. B **582** (2004) 179.
- [10] T. Herpay and P. Kovacs, Phys. Rev. D **78** (2008) 116008.
- [11] M. Matsuzaki, Phys. Rev. D **82** (2010) 016005.
- [12] J. I. Kapusta, Phys. Rev. D **24** (1981) 426.
- [13] H. E. Haber and H. A. Weldon, Phys. Rev. D **25** (1982) 502.
- [14] L. He, M. Jin, and P. Zhuang, Phys.Rev. D **71** (2005) 116001.
- [15] J. O. Andersen, Phys. Rev. D **75** (2007) 065011.
- [16] J. O. Andersen and T. Brauner, Phys. Rev. D **78** (2008) 014030.
- [17] S. Shu and J.-R. Li, J.Phys. G **34** (2007) 2727.
- [18] A. Barducci, R. Casalbuoni, G. Pettini, and L. Ravagli, Phys. Rev. D **69** (2004) 096004.
- [19] D. Ebert and K.G. Klimenko, J. Phys. G Nucl. Part. Phys. **32** (2006) 599.
- [20] D. Ebert and K.G. Klimenko, Eur. Phys. J. C **46** (2006) 771.
- [21] S. Lawley, W. Bentz, and A. W. Thomas, Phys. Lett. B **632** (2006) 495.
- [22] X. Hao and P. Zhuang, Phys.Lett. B **652** (2007) 275.
- [23] J. O. Andersen and L. T. Kyllingstad, J. Phys. G **37** (2009) 015003.
- [24] H. Abuki, R. Anglani, M. Pellicoro, and M. Ruggieri, Phys. Rev. D **79** (2009) 034032.
- [25] S. Mukherjee, M. G. Mustapha, and R. Ray, Phys Rev. D **75** (2006) 094015.
- [26] H. Abuki, M. Ciminale, R. Gatto, N.D. Ippolito, G. Nardulli, and M. Ruggieri, Phys. Rev. D **78** (2008) 014002; M. Ruggieri, Prog. Theor. Phys. Suppl.174, **60** (2008) 173.
- [27] G.-F. Sun, L. He, and P. Zhuang, Phys. Rev. D **75** (2007) 096004, e-Print: arXiv:hep-ph/0703159.
- [28] C. Wetterich, Nucl. Phys. B. **352** (1991) 529.
- [29] D. F. Litim and J. M. Pawłowski, e-Print: arXiv:hep-th/9901063.
- [30] J. Polonyi, Central Eur. J. Phys. **1** (2003) 1.
- [31] J. Berges, N. Tetradis and C. Wetterich, Phys. Rept. **363** (2002) 223.
- [32] H. Gies, e-Print: arXiv:hep-ph/0611146.

- [33] J. M. Pawłowski, *Annals Phys.* **322** (2007) 2831.
- [34] B.-J. Schaefer and J. Wambach, *Phys. Part. Nucl.* **39** (2008) 1025.
- [35] P. Kopietz, L. Bartosch, and F. Schütz, *Introduction to the Functional Renormalization group*, Springer-Verlag, Berlin Heidelberg, 2010.
- [36] O. J. Rosten, e-Print: arXiv:1003.1366 [hep-th].
- [37] E. E. Svanes, Masters' thesis NTNU 2010: *The Non-Perturbative Renormalization Group with Applications*, <http://www.nt.ntnu.no/users/jensoa/svanes.pdf>
- [38] T. R. Morris and M. D. Turner, *Nucl. Phys. B* **509** (1998) 637.
- [39] J. Berges, D.-U. Jungnickel, and C. Wetterich, *Eur. Phys. J. C* **13** (2000) 323.
- [40] B.-J. Schaefer and J. Wambach, *Nucl. Phys. A* **757** (2005) 479.
- [41] J. Braun, *Phys. Rev. D* **81** (2010) 016008.
- [42] T. K. Herbst, J. M. Pawłowski, B.-J. Schaefer, e-Print: arXiv:1008.0081 [hep-ph].
- [43] J.-P. Blaizot, A. Ipp, and N. Wschebor, e-Print: arXiv:1007.0991 [hep-ph].
- [44] J.-P. Blaizot, A. Ipp, R. Mendez-Galain, N. Wschebor, *Nucl. Phys.* **A784** (2007) 376. e-Print: arXiv:hep-ph/0610004.
- [45] F. Benitez, J.-P. Blaizot, H. Chate, N. B. Delamotte, *Phys. Rev. E* **80** (2009) 030103.
- [46] J. O. Andersen and M. Strickland, *Phys. Rev. A* **60** (1999) 1442.
- [47] D. Litim, *Phys. Rev. D* **64** (2001) 105007.
- [48] L. Canet, B. Delamotte, D. Mouhanna, and J. Vidal, *Phys. Rev. D* **67** (2003) 065004.
- [49] C. Vafa and E. Witten, *Nucl. Phys. B* **234** (1984) 173.
- [50] D.T. Son, e-Print: arXiv:hep-ph/0204199.